^{35}Cl and ^{37}Cl Magic-Angle Spinning NMR Spectroscopy in the Characterization of Inorganic Perchlorates

Jørgen Skibsted and Hans J. Jakobsen*

Instrument Centre for Solid-State NMR Spectroscopy, Department of Chemistry, University of Aarhus, DK-8000 Aarhus C, Denmark

Received October 2, 1998

^{35}Cl quadrupole coupling constants (C_Q), asymmetry parameters (η_Q), and isotropic chemical shifts (δ_{iso}) have been determined for a series of inorganic perchlorates from ^{35}Cl magic-angle spinning (MAS) NMR spectra at 14.1 T. Illustrative ^{37}Cl MAS NMR spectra are obtained and analyzed for some of the samples. For perchlorate anions with quadrupolar couplings less than about 1 MHz, the ^{35}Cl/^{37}Cl NMR parameters are most precisely determined from the full manifold of spinning sidebands observed for the satellite transitions while line-shape analysis of the central transition is employed for the somewhat larger quadrupolar couplings. The environments for the individual perchlorate anions are best characterized by the quadrupole coupling parameters (e.g., C_Q ranges from 0.3 to 3.0 MHz), while the dispersion in the isotropic ^{35}Cl chemical shifts is small (1029 ppm $< \delta_{iso} <$ 1049 ppm) for the perchlorates studied. Due to the variation in quadrupole coupling parameters, ^{35}Cl MAS NMR may conveniently be employed for identification of anhydrous and hydrated phases of perchlorates, in studies of phase transitions, hydration reactions, and the composition of mixed phases. The perchlorates studied include anhydrous $KClO_4$, $RbClO_4$, $CsClO_4$, $(CH_3)_4NClO_4$, and the anhydrous and/or hydrated forms of $LiClO_4$, $NaClO_4$, $Mg(ClO_4)_2$, $Ba(ClO_4)_2$, and $Cd(ClO_4)_2$. The ^{35}Cl MAS NMR spectra of $LiClO_4$, $Mg(ClO_4)_2$, and $Ba(ClO_4)_2$, for which the crystal structures are unknown, reveal that each of these salts possesses a single perchlorate site in the asymmetric unit. The ^{35}Cl NMR data for $Mg(ClO_4)_2$ and $Ba(ClO_4)_2$ suggest that these two samples are isostructural. Relationships between the ^{35}Cl NMR parameters and crystal symmetries are discussed for the other perchlorates where crystal structure data have been reported.

Introduction

The two naturally occurring chlorine isotopes, ^{35}Cl and ^{37}Cl, both have nuclear spin $I = {}^3/_2$ and almost identical gyromagnetic ratios and quadrupole moments. Although both isotopes are amenable to NMR experiments, the threefold-higher natural abundance for ^{35}Cl (75.53%) makes this the more attractive NMR isotope of the two. ^{35}Cl NMR has earlier been used in solution studies, utilizing the large ^{35}Cl chemical shift dispersion for the different oxidation states of the chlorine anions.[1] Furthermore, investigations of ^{35}Cl quadrupolar relaxation have provided valuable information about molecular reorientation and association processes of Cl^- and ClO_x^- ions in solution.[1]

Little attention has been paid to the application of the ^{35}Cl isotope in solid-state NMR investigations of inorganic materials. This probably reflects the fact that the relatively low ^{35}Cl gyromagnetic ratio causes the experimental difficulties associated with low-frequency NMR nuclei (e.g., acoustic probe ringing). Furthermore, for large ^{35}Cl quadrupole couplings a substantial second-order quadrupolar broadening of the central transition may hamper the observation of ^{35}Cl resonances in powdered solids. For example, the very large ^{35}Cl quadrupolar couplings for covalently bonded chlorine in organic compounds (i.e., $20 \lesssim C_Q \lesssim 80$ MHz)[2,3] imply that the ^{35}Cl quadrupolar couplings can only be determined from single-crystal NMR,[4] nuclear quadrupole resonance (NQR),[2,3,5] or static-powder NMR with the carrier frequency being incremented over the entire spectral width for the central transition.[6] For chloride ions in highly symmetric environments, the quadrupole couplings become smaller and thereby allow standard static-powder and magic-angle spinning (MAS) NMR methods to be employed. For example, this situation occurs for ^{35}Cl in chloride salts (in particular for cubic structures) and for perchlorate anions where the bonding of chlorine to four oxygens generally is close to ideal tetrahedral symmetry. This fact has been utilized in ^{35}Cl static and MAS NMR studies of cubic alkali chloride salts[7,8] and of CuCl[9] where the aim has been an investigation of the relationships between ^{35}Cl isotropic chemical shifts and the short-range structure of the salts. ^{35}Cl chemical shifts, obtained from MAS NMR spectra, have also been employed to characterize the electronic properties of Na_4Cl and Ag_4Cl clusters encapsulated in zeolites and sodalites.[10] Solid-state ^{35}Cl NMR spectra of perchlorate anions have been reported only for some methylammonium perchlorates[11] and for guanidinium perchlo-

* To whom correspondence should be addressed. Phone: +45 8942 3842. Fax: +45 8616 6199. E-mail: hja@kemi.aau.dk.

(1) Lindman, B.; Forsén, S. *NMR, Basic Principles and Progress*; Diehl, P., Fluck, E., Kosfeld, R., Eds.; Springer-Verlag: Berlin, 1976; Vol. 12.
(2) Lucken, E. A. C. *Nuclear Quadrupole Coupling Constants*; Academic Press: London, 1969.
(3) Wigand, S.; Weiden, N.; Weiss, A. *Ber. Bunsen-Ges. Phys. Chem.* **1989**, *93*, 913.
(4) Spiess, H. W.; Sheline, R. K. *J. Chem. Phys.* **1971**, *54*, 1099.
(5) (a) Gutowski, H. S.; Williams, G. A. *Phys. Rev.* **1957**, *105*, 464. (b) Green, P. J.; Graybeal, J. D. *J. Am. Chem. Soc.* **1967**, *89*, 4305.
(6) Yesinowski, J. P.; Buess, M. L.; Garroway, A. N.; Ziegeweid, M.; Pines, A. *Anal. Chem.* **1995**, *67*, 2256.
(7) Weeding, T. L.; Veeman, W. S. *J. Chem. Soc., Chem. Commun.* **1989**, 946.
(8) Hayashi, S.; Hayamizu, K. *Bull. Chem. Soc. Jpn.* **1990**, *63*, 913.
(9) Becker, K. D. *J. Chem. Phys.* **1978**, *68*, 3785.
(10) Jelinek, R.; Stein, A.; Ozin, G. A. *J. Am. Chem. Soc.* **1993**, *115*, 2390.

10.1021/ic9811650 CCC: $18.00
Published on Web 03/26/1999

rate.[12] Both studies employ variable-temperature NMR to investigate the temperature dependence of the quadrupole coupling parameters (C_Q and η_Q) or the T_1 spin−lattice relaxation time, providing information about the molecular motions of the ClO_4^- anions in the tri-, di-, and monomethylammonium perchlorates and the solid−solid-phase transition at 452 K for guanidinium perchlorate.

In this work we utilize the combination of a high magnetic field (14.1 T) and magic-angle spinning to observe the ^{35}Cl (and ^{37}Cl) central and satellite transitions for a series of inorganic perchlorates. In addition to an increase in sensitivity, the high magnetic field decreases the second-order quadrupolar broadening and the effects of acoustic ringing. These factors are specifically important for the observation of reliable intensities for the spinning sidebands (ssbs) from the satellite transitions. As demonstrated earlier for other half-integer spin nuclei,[13] the full manifold of ssbs from the satellite transitions provides a valuable tool for obtaining a precise determination of the quadrupole coupling parameters for spin $I = {}^3/_2$ nuclei possessing relatively small quadrupolar interactions (i.e., $C_Q \lesssim 1$ MHz).

The perchorates studied in this work include anhydrous and hydrated salts of the alkali metals (Li, K, Na, Rb, and Cs) and of the divalent metal ions Mg^{2+}, Ba^{2+}, and Cd^{2+}. The aim of this work has been to obtain precise values for the ^{35}Cl quadrupole coupling parameters and isotropic chemical shifts for these samples and to illustrate that anhydrous and hydrated phases of perchlorates can readily be distinguished and characterized using the ^{35}Cl quadrupole coupling parameters. To our knowledge, ^{35}Cl quadrupolar couplings for perchlorates in the solid state are reported in only two cases, i.e., for trimethylammonium perchlorate ($C_Q = 0.318$ MHz and $\eta_Q = 0.6$)[11] and guanidinium perchlorate ($C_Q = 1.48$ MHz and $\eta_Q = 0.6$)[12] at ambient temperature. Such values may form a valuable basis for future applications of ^{35}Cl MAS NMR in coordination chemistry, for example in studies of perchlorates used as counterions or ligands in organometallic complexes.

Experimental Section

Solid-state ^{35}Cl and ^{37}Cl MAS NMR spectra were recorded on a wide-bore Varian INOVA-600 spectrometer (14.1 T) at 58.84 and 48.98 MHz, respectively, using a multinuclear 7-mm CP/MAS probe from Doty Scientific Inc. This probe allowed spinning speeds up to approximately 10 kHz to be employed, and high-stability spinning (±1 Hz) was achieved using the Varian rotor-speed controller. All experiments were performed at ambient temperature with exact magic-angle setting (54.74 ± 0.02°), spectral widths in the range 0.1−1.0 MHz, single-pulse excitation with pulse widths of 0.5−2.0 μs ($\gamma B_1/2\pi \approx 31$ kHz for ^{35}Cl and $\gamma B_1/2\pi \approx 25$ kHz for ^{37}Cl), and relaxation delays of 1−2 s. The magic angle was initially adjusted by minimizing the line widths for the ssbs from the ^{79}Br satellite transitions for KBr. Exact setting was subsequently obtained by finally minimizing the line widths for the ssbs from the ^{35}Cl satellite transitions for $Ba(ClO_4)_2$ (vide infra). Good MAS NMR signal-to-noise ratios were generally obtained using 4096 and 16 384 scans for the central and satellite transitions, respectively. Baseline distortions were suppressed by linear prediction of the first few (5−20) data points of the FID using the numerical procedure described by Barkhuijsen et al.[14] which has been implemented into the Varian VNMR software. Following the linear prediction the spectra were baseline corrected using the Varian VNMR routine.

Table 1. ^{35}Cl Quadrupole Coupling Constants (C_Q), Asymmetry Parameters (η_Q), and Isotropic Chemical Shifts (δ_{iso}) for Alkali-Metal and Divalent Metal Perchlorates[a]

compound	C_Q (MHz)	η_Q	δ_{iso} (ppm)[b]
$LiClO_4$	1.282 ± 0.008	0.34 ± 0.01	1034.2 ± 0.5
$LiClO_4 \cdot 3H_2O$	0.695 ± 0.004	0.00 ± 0.03	1045.9 ± 0.5
$NaClO_4$	0.887 ± 0.014	0.92 ± 0.02	1044.3 ± 0.5
$NaClO_4 \cdot H_2O$	0.566 ± 0.009	0.90 ± 0.02	1039.9 ± 0.3
$KClO_4$	0.440 ± 0.006	0.88 ± 0.02	1049.2 ± 0.3
$RbClO_4$	0.537 ± 0.015	0.87 ± 0.03	1049.4 ± 0.3
$CsClO_4$	0.585 ± 0.008	0.86 ± 0.02	1047.7 ± 0.3
$Mg(ClO_4)_2$	2.981 ± 0.007	0.57 ± 0.01	1036.2 ± 0.5
$Mg(ClO_4)_2 \cdot 6H_2O$			
Cl(1)	0.309 ± 0.006	0.00 ± 0.08	1046.6 ± 0.3
Cl(2)	0.475 ± 0.008	0.00 ± 0.05	1045.5 ± 0.3
$Ba(ClO_4)_2$	2.256 ± 0.008	0.58 ± 0.01	1029.6 ± 0.5
$Ba(ClO_4)_2 \cdot 3H_2O$	0.383 ± 0.005	0.00 ± 0.03	1040.6 ± 0.3
$Cd(ClO_4)_2 \cdot 6H_2O$	0.328 ± 0.005	0.00 ± 0.03	1044.4 ± 0.3
$(CH_3)_4NClO_4$	0.307 ± 0.004	0.00 ± 0.03	1049.3 ± 0.3

[a] The error limits for C_Q and η_Q are 95% confidence limits calculated numerically using the method described in ref 15. [b] Isotropic chemical shifts are relative to ^{35}Cl in an external sample of solid NaCl.

Isotropic chemical shifts (Tables 1 and 2) are relative to the ^{35}Cl and ^{37}Cl resonances of solid NaCl. However, in the figures of the MAS NMR spectra for the satellite transitions, the kilohertz scale is given relative to the center of gravity for the central transition in order to appreciate the symmetry of the ssb manifolds.

Simulations, least-squares fitting, and numerical error analysis of the experimental spectra were performed on a SUN ULTRA 1 workstation (linked to the INOVA-600 spectrometer) using the solid-state NMR software package STARS[13,15,16] developed in our laboratory, incorporated into the Varian VNMR software, and presently available as part of Varian's solid-state NMR package. The simulation program calculates the contributions from the first- and second-order average Hamiltonians for the quadrupole interaction in the secular approximation. The effect from nonuniform detection (i.e., the quality factor Q of the probe)[13] has been included in the simulations using a Q factor of 80 for the 7-mm CP/MAS probe employed in this work. Intensity distortions caused by nonideal excitation[13] are found to be negligible for the spin systems considered here (short pulse widths) and have not been considered in the simulations. The error limits (95% confidence intervals) for the optimized quadrupole coupling parameters have been calculated by the method of numerical error analysis described elsewhere.[15]

Samples of anhydrous $LiClO_4$, $KClO_4$, $RbClO_4$, and $CsClO_4$ and the hydrates $NaClO_4 \cdot H_2O$, $Mg(ClO_4)_2 \cdot 6H_2O$, $Ba(ClO_4)_2 \cdot 3H_2O$, and $Cd(ClO_4)_2 \cdot 6H_2O$ are commercially available and were studied as received. $NaClO_4$ was prepared by heating the monohydrate at 160 °C overnight, and the purity of this phase as well as that of $NaClO_4 \cdot H_2O$ was confirmed by ^{23}Na MAS NMR, which gave quadrupole coupling and chemical shift data in accordance with those reported recently for these phases.[17] Since $LiClO_4$ readily absorbs water, a pure sample of anhydrous $LiClO_4$ was prepared by heating the commercial sample at 150 °C overnight. The trihydrate, $LiClO_4 \cdot 3H_2O$, was obtained by exposure of $LiClO_4$ to a humid atmosphere in a desiccator for 1 day. Anhydrous $Mg(ClO_4)_2$ and $Ba(ClO_4)_2$ were obtained by heating the corresponding hydrates overnight at 120 and 160 °C, respectively. The two anhydrates were handled in a glovebox to keep the hydration of these phases to a minimum. Phase identification and purity tests of the anhydrous and hydrated lithium, magnesium, and barium perchlorates were performed using powder X-ray diffraction, differential thermal analysis (DTA), and thermogravimetric analysis (TGA).

(11) Jurga, S.; Harbison, G. S.; Blümich, B.; Spiess, H. W. *Ber. Bunsen-Ges. Phys. Chem.* **1986**, *90*, 1153.
(12) Furukawa, Y.; Ikeda, R. *Ber. Bunsen-Ges. Phys. Chem.* **1993**, *97*, 1143.
(13) Skibsted, J.; Nielsen, N. C.; Bildsøe, H.; Jakobsen, H. J. *J. Magn. Reson.* **1991**, *95*, 88.
(14) Barkhuijsen, H.; De Beer, R.; Bovée, W. M. M. J.; van Ormondt, D. *J. Magn. Reson.* **1985**, *61*, 465.
(15) Skibsted, J.; Vosegaard, T.; Bildsøe, H.; Jakobsen, H. J. *J. Phys. Chem.* **1996**, *100*, 14872.
(16) (a) Skibsted, J.; Nielsen, N. C.; Bildsøe, H.; Jakobsen, H. J. *Chem. Phys. Lett.* **1992**, *188*, 405. (b) Vosegaard, T.; Skibsted, J.; Bildsøe, H.; Jakobsen, H. J. *J. Phys. Chem.* **1995**, *99*, 10731.
(17) Koller, H.; Engelhardt, G.; Kentgens, A. P. M.; Sauer, J. *J. Phys. Chem.* **1994**, *98*, 1544.

Table 2. ^{37}Cl Quadrupole Coupling Constants (C_Q), Asymmetry Parameters (η_Q), and Isotropic Chemical Shifts (δ_{iso}) for Selected Inorganic Perchlorates[a]

compound	C_Q (MHz)	η_Q	$C_Q(^{35}Cl)/C_Q(^{37}Cl)$[b]	δ_{iso} (ppm)[c]
$LiClO_4$	1.010 ± 0.012	0.34 ± 0.01	1.27 ± 0.02	1034.1 ± 0.5
$NaClO_4 \cdot H_2O$	0.459 ± 0.012	0.91 ± 0.04	1.23 ± 0.05	1040.1 ± 0.5
$RbClO_4$	0.424 ± 0.014	0.86 ± 0.02	1.27 ± 0.07	1049.1 ± 0.3
$Mg(ClO_4)_2 \cdot 6H_2O$				
Cl(1)	0.245 ± 0.005	0.00 ± 0.10	1.26 ± 0.05	1046.6 ± 0.3
Cl(2)	0.375 ± 0.003	0.00 ± 0.07	1.27 ± 0.03	1045.5 ± 0.3
$Ba(ClO_4)_2 \cdot 3H_2O$	0.299 ± 0.004	0.01 ± 0.03	1.28 ± 0.03	1040.5 ± 0.5

[a] The error limits for C_Q and η_Q are 95% confidence limits calculated numerically using the method described in ref 15. [b] $C_Q(^{35}Cl)/C_Q(^{37}Cl)$ ratios calculated using the $C_Q(^{35}Cl)$ values in Table 1. [c] Isotropic chemical shifts are relative to ^{37}Cl in an external sample of solid NaCl.

CAUTION! Since perchlorates are powerful oxidizers, they are potentially hazardous, especially in contact with reducing materials.[18] Furthermore, they may explode when exposed to shock or heat.[18] Thus, any contact of the perchlorate samples with organic materials was avoided during sample packing into the airtight rotors. To test the shock and thermal (frictional heating) stability of the perchlorate samples prior to the NMR experiments, the packed rotors were bench tested for safe sample spinning up to 9.0 kHz. In some cases, the samples were also tested by heating to temperatures about 100−150 °C prior to packing of the rotors.

Results and Discussion

The determination of the ^{35}Cl quadrupole coupling parameters and isotropic chemical shifts from ^{35}Cl MAS NMR spectra of either the satellite or central transitions is described below for the individual perchlorates. For those perchlorates where crystal structure data are available, the results from ^{35}Cl MAS NMR are discussed with respect to the point symmetries of the chlorine sites. In the final part, illustrative ^{37}Cl MAS NMR spectra for some of the perchlorates are presented. The ^{35}Cl and ^{37}Cl quadrupole coupling parameters and isotropic chemical shifts, determined from the MAS NMR spectra, are summarized in Tables 1 and 2, respectively.

$KClO_4$, $RbClO_4$, and $CsClO_4$. For the alkali-metal perchlorates, the crystal structures reveal that $KClO_4$, $RbClO_4$, and $CsClO_4$ are isostructural and belong to the orthorhombic space group *Pnma*.[19,20] This fact is clearly reflected in their ^{35}Cl MAS NMR spectra (Figure 1a−c) since strong similarities between the ssb manifolds for the satellite transitions and between the second-order quadrupolar line shapes for the central transition are observed for these three perchlorates. Although simulations of the second-order quadrupolar line shapes, observed for the central transitions (Figure 1a−c), allow determination of the ^{35}Cl quadrupole coupling parameters, we observe as in other cases that higher precisions for these parameters are achieved by least-squares fitting of simulated to experimental ssb intensities for the satellite transitions. Following this approach gives the C_Q and η_Q values listed in Table 1 for the three isostructural perchlorates while the isotropic chemical shifts (δ_{iso}) are obtained from the center of gravity of the satellite transitions after correction for the second-order quadrupolar induced shift.[13,21,22] As an example of the excellent agreement between the simulated and experimental manifolds of ssbs, Figure 1d illustrates the simulated spectrum of the satellite transitions for $CsClO_4$. The optimized NMR parameters in Table 1 show that for $KClO_4$, $RbClO_4$, and $CsClO_4$ the ^{35}Cl sites are best characterized/distinguished by their quadrupole coupling constant since their asymmetry parameters and isotropic chemical shifts are almost identical. Somewhat larger dispersions in

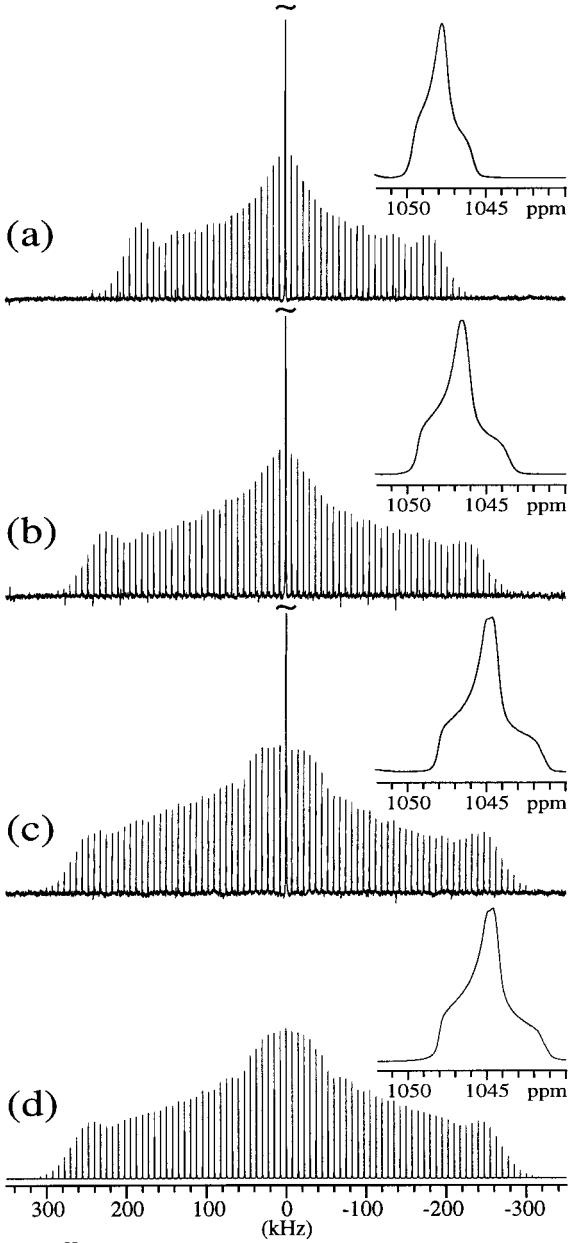

Figure 1. ^{35}Cl MAS NMR spectra of the central and satellite transitions for (a) $KClO_4$, (b) $RbClO_4$, and (c) $CsClO_4$, recorded at $\nu_L = 58.84$ MHz (14.1 T) using a spinning speed of $\nu_r = 7500$ Hz and 16 384 scans. (d) Simulated spectra of the central and satellite transitions for $CsClO_4$ corresponding to the optimized C_Q and η_Q values listed in Table 1. The resonance for the central transition in panels a−c is cut off at approximately $^1/_{12}$ of its total height. The insets for the central transitions illustrate their second-order quadrupolar line shapes on a ppm scale, relative to ^{35}Cl in solid NaCl.

(18) Sax, N. I.; Lewis, R. J. *Dangerous Properties of Industrial Materials*, 7th ed.; Van Nostrand Reinhold: New York, 1989; Vol. 3.
(19) Johansson, G. B.; Lindqvist, O. *Acta Crystallogr.* **1977**, *33B*, 2918.
(20) Granzin, J. *Z. Kristallogr.* **1988**, *184*, 157.
(21) Samoson A. *Chem. Phys. Lett.* **1985**, *119*, 29.
(22) Jakobsen, H. J.; Skibsted, J.; Bildsøe, H.; Nielsen, N. C. *J. Magn. Reson.* **1989**, *85*, 173.

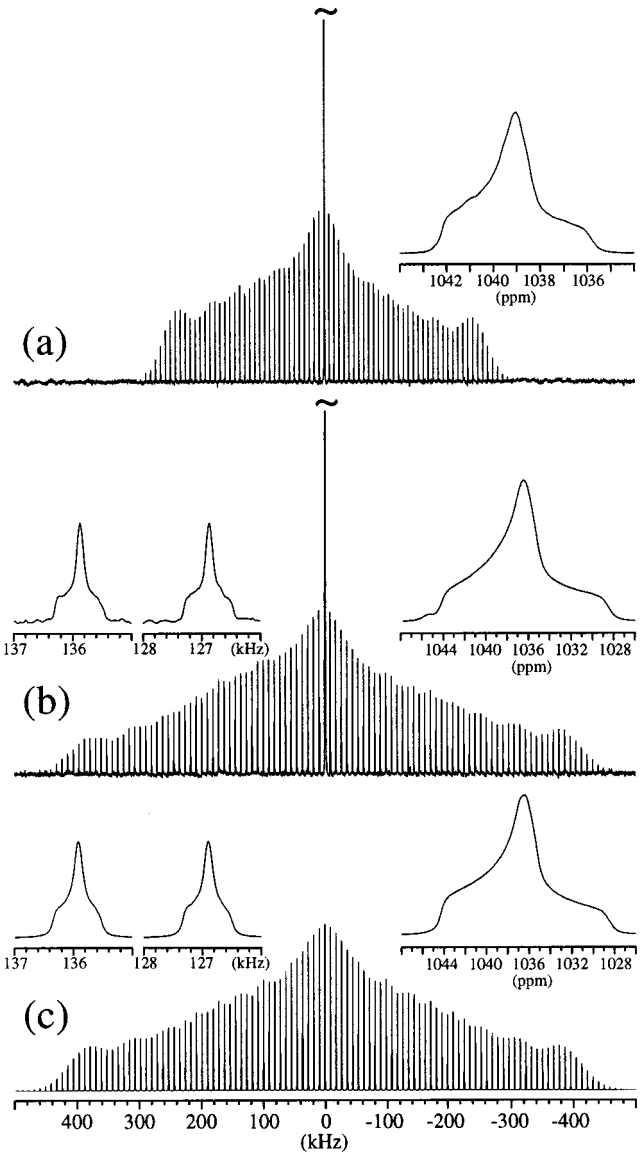

Figure 2. ^{35}Cl MAS NMR spectra of the satellite transitions for (a) $NaClO_4 \cdot H_2O$ and (b) $NaClO_4$, recorded using spinning speeds of 8.0 and 9.0 kHz, respectively. The resonance from the central transition in panels a and b is cut off at approximately $^1/_{15}$ of its total height; however, the right-hand-side expansions illustrate the line shape for the central transition. The left-hand expansions in panel b show the second-order quadrupolar line shapes observed for two individual ssbs within the ssb manifold from the satellite transitions. (c) Simulation of the spectrum in panel b employing the optimized NMR parameters for $NaClO_4$ in Table 1. The insets in panel c illustrate expansions corresponding to those shown in panel b.

^{35}Cl chemical shifts have been reported for the three isostructural Na, K, and Rb chlorides of cubic symmetry (i.e., -46 ppm $\leq \delta_{iso} \leq 44$ ppm).[7] The smaller variation in δ_{iso} for the alkali-metal perchlorates, as compared to the corresponding chloride salts, may be related to the longer cation to chlorine distances for the perchlorates.

$NaClO_4 \cdot H_2O$ and $NaClO_4$. ^{35}Cl MAS NMR spectra of the satellite transitions for $NaClO_4 \cdot H_2O$ and $NaClO_4$ are shown in Figure 2, panels a and b, respectively, and illustrate the presence of a single ^{35}Cl site in the asymmetric unit for both phases, in agreement with the reported crystal structures.[23,24] The spectral widths for the manifolds of ssbs (equal to C_Q for spin $I = ^3/_2$ spin nuclei) show that the ^{35}Cl site for the anhydrous form possesses a somewhat larger quadrupole coupling compared to $NaClO_4 \cdot H_2O$. However, the similarity in the envelopes of the ssbs indicates that the ^{35}Cl resonances for the two phases exhibit almost the same asymmetry parameter. These observations are confirmed by the result from least-squares optimization of simulated to experimental ssb intensities for the two ssb manifolds in that $\eta_Q \approx 0.90$ is obtained for both sodium perchlorates (cf. Table 1). The left-hand-side insets of Figure 2b illustrate that second-order quadrupolar line shapes are observed for the individual ssbs of the manifold for $NaClO_4$ and that these line shapes closely resemble the line shape for the central transition as expected from theoretical considerations.[21,25] Furthermore, the ssb line shapes are clearly reproduced in the simulated ssb pattern shown in Figure 2c, which employs the optimized NMR data for $NaClO_4$ in Table 1.

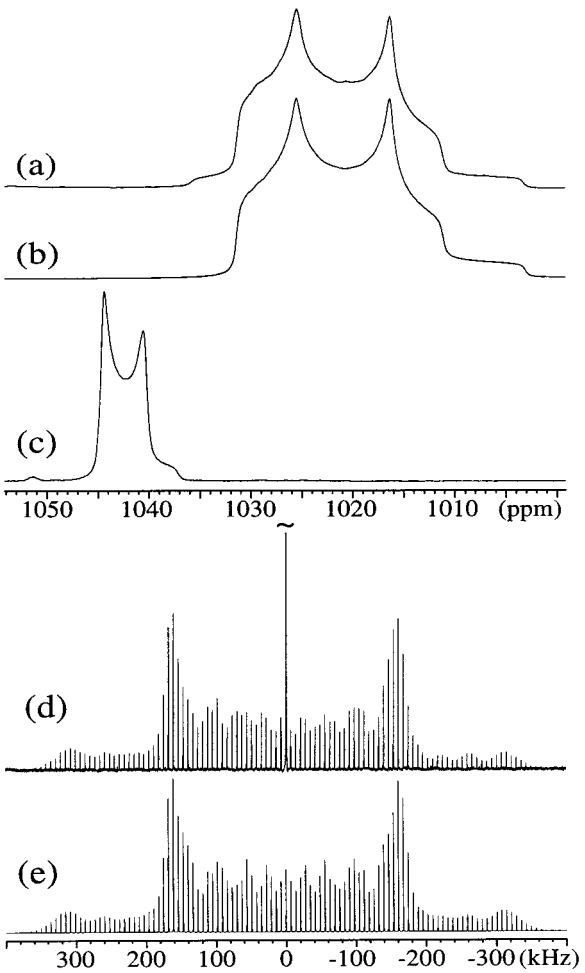

Figure 3. ^{35}Cl MAS NMR spectra of the central transition for (a) $LiClO_4$ ($\nu_r = 8.0$ kHz) and (c) $LiClO_4 \cdot 3H_2O$ ($\nu_r = 7.0$ kHz). (b) Simulation of the second-order quadrupolar line shape in panel a corresponding to the C_Q, η_Q, and δ_{iso} values in Table 1 for $LiClO_4$. (d) ^{35}Cl MAS NMR spectrum ($\nu_r = 7.0$ kHz) of the satellite transitions for $LiClO_4 \cdot 3H_2O$ shown with the central transition cut off at approximately $^1/_8$ of its total height. (e) Simulation of the ssb manifold in panel d employing the optimized NMR parameters for $LiClO_4 \cdot 3H_2O$ in Table 1.

$LiClO_4$ and $LiClO_4 \cdot 3H_2O$. ^{35}Cl MAS NMR spectra of the central transitions for $LiClO_4$ and $LiClO_4 \cdot 3H_2O$ are shown in Figure 3, panels a and c, respectively. The spectra reveal that both phases contain a single chlorine site in the asymmetric

(23) Wartchow, R.; Berthold, H. J. *Z. Kristallogr.* **1978**, *147*, 307.
(24) Berglund, B.; Thomas, J. O.; Tellgren, R. *Acta Crystallogr.* **1975**, *B31*, 1842.
(25) Skibsted, J.; Norby, P.; Bildsøe, H.; Jakobsen, H. J. *Solid State Nucl. Magn. Reson.* **1995**, *5*, 239.

unit. This observation agrees with the XRD structure determined for the trihydrate[26] while the crystal structure for $LiClO_4$ has not been reported. The larger ^{35}Cl quadrupole coupling observed for $LiClO_4$ implies that the C_Q, η_Q, and δ_{iso} values are most conveniently determined by least-squares fitting to the line shape of the central transition for this phase. An improved precision of the ^{35}Cl NMR parameters is obtained for the trihydrate by optimization to the ssb intensities observed for the satellite transitions (Figure 3d) as compared to line-shape simulations of the central transition. This holds especially for nearly axially symmetric EFG tensors since the line shape of the central transition is less sensitive to variations in η_Q for the range $0.0 \lesssim \eta_Q \lesssim 0.15$ as compared to the manifold of ssbs from the satellite transitions. The C_Q, η_Q, and δ_{iso} values obtained from least-squares optimization to the ssb intensities for $LiClO_4 \cdot 3H_2O$ (Figure 3d) are given in Table 1 and used for the simulations of the satellite transitions shown in Figure 3e. The observation of an axially symmetric EFG tensor for $LiClO_4 \cdot 3H_2O$ is in accord with the crystal structure reported for this phase (hexagonal, space group $P6_3mc$),[26] which includes a chlorine site situated on a threefold axis. The ClO_4^- ion of $LiClO_4 \cdot 3H_2O$ possesses almost ideal tetrahedral symmetry in that (i) the Cl−O bond along the threefold axis is only 0.001 Å longer than the remaining Cl−O bonds and (ii) all O−Cl−O bond angles deviate by less than 0.3° from the ideal tetrahedral angle.[26] This may indicate that the ^{35}Cl quadrupole coupling mainly reflects perturbations of the further distant coordination spheres such as the water molecules of the $Li(H_2O)_6^+$ groups coordinating to the ClO_4^- ions by hydrogen bonds. The δ_{iso} value for the trihydrate is very similar to those observed for the other alkaline metal perchlorates (cf. Table 1) which are observed over a small spectral range (i.e., 1045−1050 ppm). However, the resonance for the anhydrous phase is shifted significantly to higher shielding and possesses the largest quadrupole coupling of the studied alkali-metal perchlorates. Thus, we predict the crystal structure for $LiClO_4$ to deviate from the structure of the K, Rb, and Cs perchlorates.

$Mg(ClO_4)_2 \cdot 6H_2O$. The ^{35}Cl MAS NMR spectrum of the central transition for $Mg(ClO_4)_2 \cdot 6H_2O$ (Figure 4a) reveals the presence of two different Cl sites which exhibit almost identical chemical shifts but slightly different quadrupole couplings. The presence of two different Cl sites in $Mg(ClO_4)_2 \cdot 6H_2O$ is not immediately apparent from the manifold of ssbs, observed from the satellite transitions (Figure 4c), since the individual ssbs exhibit Gaussian-like line shapes with line widths of approximately 2 ppm. However, the overall ssb manifold cannot be simulated assuming the presence of only a single set of C_Q and η_Q parameters. Line-shape analysis of the central transitions reveals that the two resonances have a 1:1 intensity ratio and indicates the both sites are in axially symmetric environments. The C_Q and η_Q parameters determined from the central transition have been further refined by simulations of the overlapping manifolds of ssbs from the satellite transitions. This results in the final parameters listed in Table 1 and the simulated spectra of the central and satellite transitions shown in Figure 4b and Figure 4d, respectively. $Mg(ClO_4)_2 \cdot 6H_2O$ belongs to an isomorphous series of divalent metal perchlorate hexahydrates ($M(ClO_4) \cdot 6H_2O$, M = Mg, Mn, Fe, Co, Ni, Zn)[27] which have an orthorhombic structure ($Pmn2_1$).[27−29] The crystal structure for these hexahydrates resembles that of $LiClO_4 \cdot 3H_2O$ (hexagonal $P6_3mc$)[26] in that the arrangement of perchlorate anions and water molecules is identical when the metal atoms are not considered. For $Mg(ClO_4)_2 \cdot 6H_2O$, the magnesium ions occupy one-half of the cation sites available in the $LiClO_4 \cdot 3H_2O$ structure, forming alternate rows of $Mg(H_2O)_6$ octahedra. This reduces the symmetry for $Mg(ClO_4)_2 \cdot 6H_2O$ from hexagonal $P6_3mc$ to orthorhombic $Pmn2_1$, which may account for the presence of two different Cl sites in the asymmetric unit.

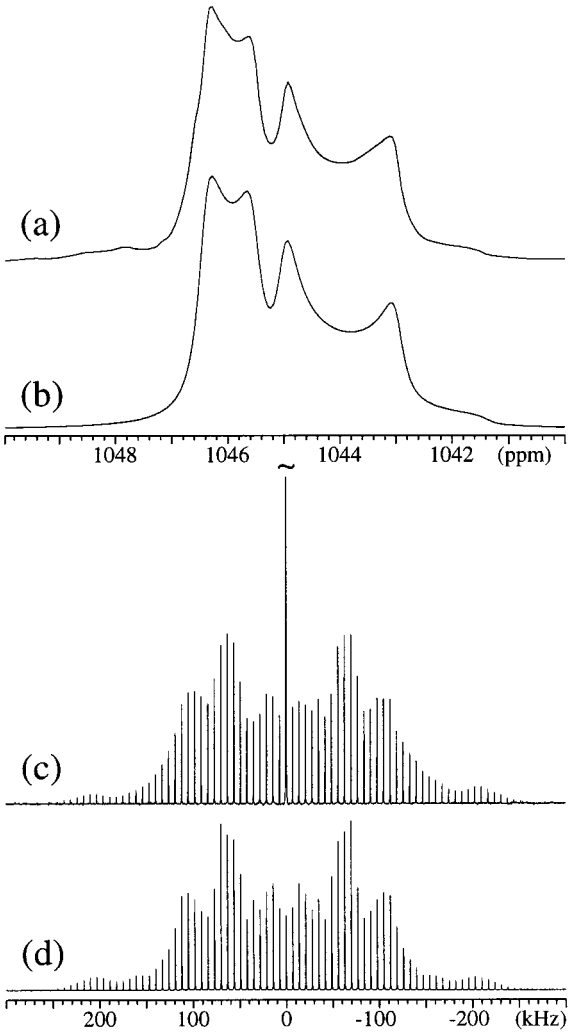

Figure 4. ^{35}Cl MAS NMR spectra of (a) the central transition and (c) the satellite transitions for $Mg(ClO_4)_2 \cdot 6H_2O$, recorded using a spinning speed of $\nu_r = 7.0$ kHz. The central transition is cut off at $^1/_{10}$ of its total height in panel c. Simulated spectra of the central and satellite transitions for the overlapping resonances from the two ClO_4^- sites are shown as 1:1 additions in panels b and d, respectively, and correspond to the ^{35}Cl NMR data listed in Table 1 for $Mg(ClO_4)_2 \cdot 6H_2O$.

$Ba(ClO_4)_2 \cdot 3H_2O$ and $Cd(ClO_4)_2 \cdot 6H_2O$. The ^{35}Cl MAS NMR spectra of the satellite transitions for $Ba(ClO_4)_2 \cdot 3H_2O$ and $Cd(ClO_4)_2 \cdot 6H_2O$ (Figure 5, panels a and c, respectively) both exhibit the appearance characteristic of a ^{35}Cl nucleus in an axially symmetric environment. The ^{35}Cl MAS spectra both exhibit an exceptionally high degree of resolution, compared to the other manifolds of ^{35}Cl ssbs reported in this work, in that the ssbs exhibit extremely narrow line widths of 0.7 ppm ($Ba(ClO_4)_2 \cdot 3H_2O$) and 1.0 ppm ($Cd(ClO_4)_2 \cdot 6H_2O$) at 14.1 T. Since these line widths are very sensitive to an exact setting of the magic angle, both perchlorates represent useful samples for accurate setting of the magic angle in MAS NMR of ^{35}Cl or other nuclei with low gyromagnetic ratios. This has been utilized

(26) Sequeira, A.; Bernal, I.; Brown, I. D.; Faggiani, R. *Acta Crystallogr.* **1975**, *B31*, 1735.
(27) West, C. D. *Z. Kristallogr.* **1935**, *91*, 480.
(28) Ghosh, M.; Ray, S. *Z. Kristallogr.* **1977**, *145*, 146.
(29) Ghosh, M.; Ray, S. *Z. Kristallogr.* **1981**, *155*, 129.

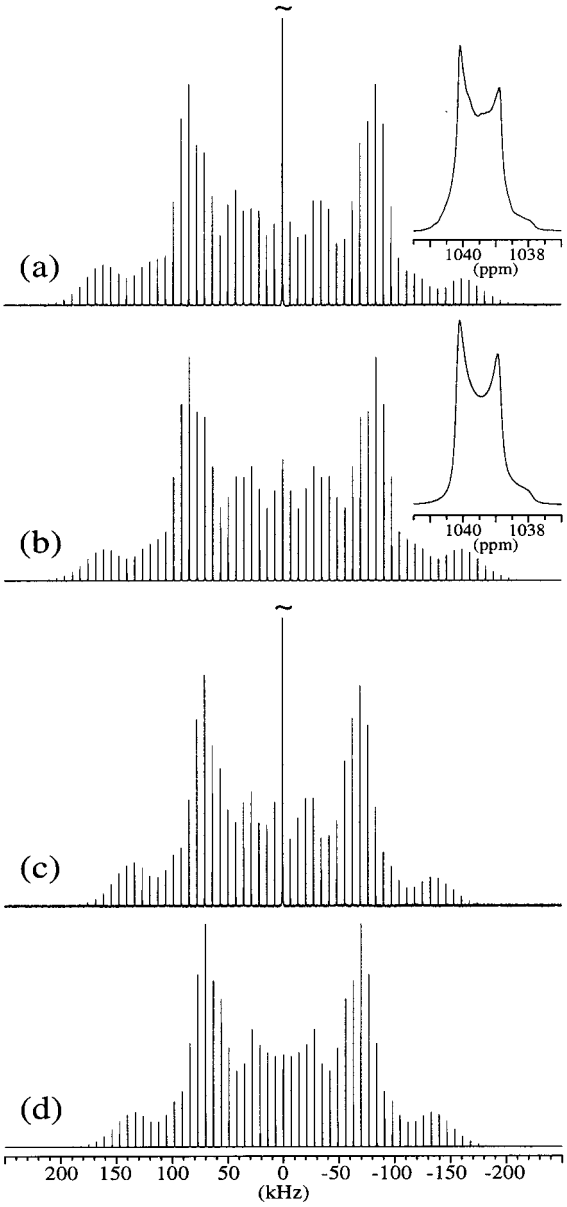

Figure 5. ^{35}Cl MAS NMR spectra (ν_r = 7.0 kHz) of the satellite transitions for (a) $Ba(ClO_4)_2 \cdot 3H_2O$ and (c) $Cd(ClO_4)_2 \cdot 6H_2O$ shown with the central transition cut off at approximately $^1/_{10}$ of its total height. The inset in panel a illustrates the line shape for the central transition for $Ba(ClO_4)_2 \cdot 3H_2O$. Simulated spectra of the ssb manifolds from the satellite transitions are shown in panels b and d for $Ba(ClO_4)_2 \cdot 3H_2O$ and $Cd(ClO_4)_2 \cdot 6H_2O$, respectively, and employ the ^{35}Cl NMR parameters in Table 1. A simulation of the central transition for $Ba(ClO_4)_2 \cdot 3H_2O$ is shown as the inset in panel b.

in this work where the magic angle is optimized by minimizing the line width of ssbs from the satellite transitions for $Ba(ClO_4)_2 \cdot 3H_2O$. The high degree of resolution is also reflected in the ^{35}Cl MAS spectrum of the central transition for $Ba(ClO_4)_2 \cdot 3H_2O$ (inset of Figure 5a), where a well-defined second-order quadrupolar line shape is observed with a frequency difference for the two singularities ("horns") as low as 1.2 ppm. The quadrupole coupling parameters (Table 1), obtained from fitting of simulated to the experimental manifolds of ssbs in Figure 5a and Figure 5c, reveal that the ^{35}Cl sites in $Ba(ClO_4)_2 \cdot 3H_2O$ and $Cd(ClO_4)_2 \cdot 6H_2O$ are in axially symmetric environments ($\eta_Q = 0$) and that the two phases possess the smallest quadrupolar couplings observed for the inorganic perchlorates examined in this work. The axial symmetry of the quadrupole coupling tensors is in accord with the crystal structures determined earlier

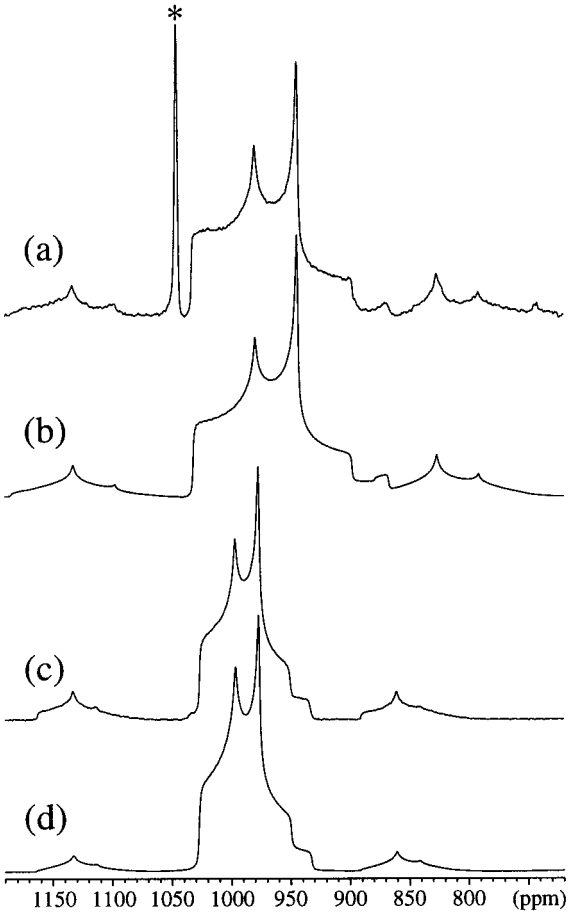

Figure 6. ^{35}Cl MAS NMR spectra of the central transitions for (a) $Mg(ClO_4)_2$ and (c) $Ba(ClO_4)_2$ recorded using spinning speeds of 9.0 and 8.0 kHz, respectively. The asterisk in panel a indicates the resonance from a minor impurity of the hydrated phase, $Mg(ClO_4)_2 \cdot 6H_2O$. Simulated spectra of the central transitions for $Mg(ClO_4)_2$ and $Ba(ClO_4)_2$ are shown in panels b and d, respectively, and employ the C_Q, η_Q, and δ_{iso} values for these two perchlorates listed in Table 1.

by XRD.[30,31] These show that $Ba(ClO_4)_2 \cdot 3H_2O$ has a hexagonal structure ($P6_3/m$)[30] while $Cd(ClO_4)_2 \cdot 6H_2O$ belongs to the trigonal space group $P\bar{3}m1$.[31] The low value for the ^{35}Cl quadrupole coupling constant for $Cd(ClO_4)_2 \cdot 6H_2O$ may reflect the fact that the ClO_4^- anions are coordinated by only loose hydrogen bonds between the strings of $Cd(H_2O)_6$ octahedra in the structure of $Cd(ClO_4)_2 \cdot 6H_2O$.[31] This results in a configuration with only slight distortion of the tetrahedral symmetry for the ClO_4^- anion. The crystal structure for $Ba(ClO_4)_2 \cdot 3H_2O$ is composed of columns of Ba−O icosahedra linked together through ClO_4^- anions each of which participates in three different icosahedra.[30] This arrangement results in a nearly ideal tetrahedral geometry for the ClO_4^- anion, which may account for the small quadrupole coupling determined for this phase.

$Mg(ClO_4)_2$ and $Ba(ClO_4)_2$. The anhydrous phases of magnesium and barium perchlorate are extremely hygroscopic and readily form the hydrated phases, $Mg(ClO_4)_2 \cdot 6H_2O$ and $Ba(ClO_4)_2 \cdot 3H_2O$, if they are exposed to a humid atmosphere for a few minutes. This may account for the fact that crystal structures have only been reported for the hydrated phases of these perchlorates. Experimental ^{35}Cl MAS NMR spectra of the central transition for the anhydrous phases of $Mg(ClO_4)_2$ and $Ba(ClO_4)_2$ are shown in Figure 6, panels a and c, respectively.

(30) Gallucci, J. C.; Gerkin, R. E. *Acta Crystallogr.* **1988**, *C44*, 1873.
(31) Johansson, G.; Sandström, M. *Acta Chem. Scand.* **1987**, *A41*, 113.

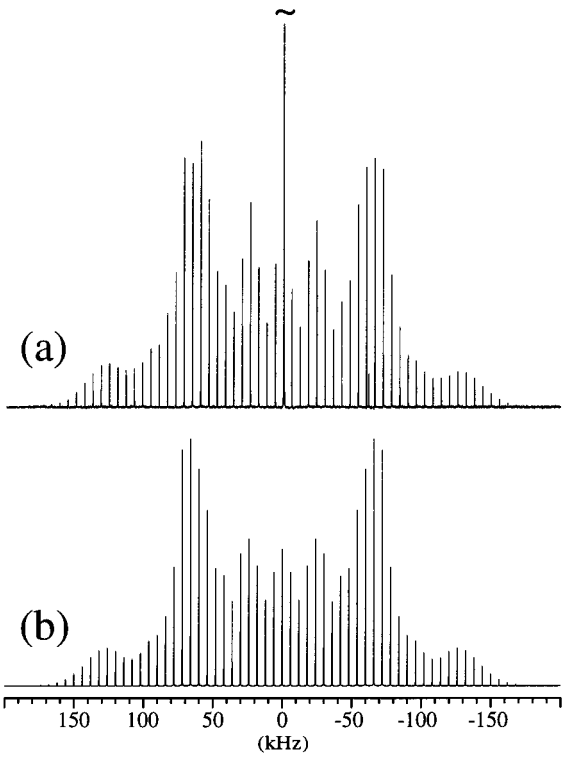

Figure 7. (a) ^{35}Cl MAS NMR spectrum ($\nu_r = 6.0$ kHz) of the central and satellite transitions for $(CH_3)_4NClO_4$ shown with the central transition cut off at $^1/_{10}$ of its total height. (b) Simulated spectrum of the satellite transitions corresponding to the quadrupole coupling parameters for $(CH_3)_4NClO_4$ listed in Table 1.

These second-order spectra reveal the presence of a single perchlorate site in the asymmetric unit for both phases and that the ^{35}Cl quadrupolar couplings are significantly larger than those determined for the hydrated forms. Simulated spectra of the central transition for $Mg(ClO_4)_2$ and $Ba(ClO_4)_2$, using the optimized parameters in Table 1, are illustrated in Figure 6, panels b and d, respectively, and are seen to reproduce all spectral features of the experimental line shapes for the centerband and the first ssbs from the central transitions in Figure 6a,c. The C_Q, η_Q, and δ_{iso} values obtained from these simulations (Table 1) show that the two phases exhibit nearly identical asymmetry parameters and chemical shifts, the latter being shifted to higher shielding as compared to those for the hydrated phases. This indicates the presence of very similar symmetries and geometries for the perchlorate anions in the asymmetric units of $Mg(ClO_4)_2$ and $Ba(ClO_4)_2$, which may suggest that these two perchlorates are isostructural compounds. The considerably larger quadrupolar couplings for the anhydrous phases as compared to the hydrated forms may reflect a direct coordination of the ClO_4^- anions to the Mg^{2+} and Ba^{2+} cations. Such arrangements are expected to result in more distorted environments for the ClO_4^- anions as compared to the structures for the hydrates where the cations are mainly coordinated to water molecules forming units which are linked together by hydrogen-bonded ClO_4^- anions.

$(CH_3)_4NClO_4$. As a final application of ^{35}Cl MAS NMR to perchlorates, Figure 7a shows the spectrum of the satellite transitions for tetramethylammonium perchlorate, $(CH_3)_4NClO_4$. The individual ssbs of this manifold exhibit a narrow line width of 1.0 ppm, i.e., line widths of the same magnitude as those observed for the barium and cadmium perchlorate hydrates (cf. Figure 5). The ^{35}Cl quadrupole coupling parameters (Table 1), obtained from the ssbs in Figure 7a and illustrated by the optimized simulation for the satellite transitions in Figure 7b, reveal the smallest quadrupole coupling determined in this study and a chlorine site in an axially symmetric environment. The latter agrees with the crystal structure reported for $(CH_3)_4NClO_4$ (tetragonal, *P*4/*nmm*)[32] in which the perchlorate anion possesses regular tetrahedral symmetry within the error limits of the observed positional parameters. The isotropic chemical shift observed for $(CH_3)_4NClO_4$ ($\delta_{iso} = 1049$ ppm) is very similar to the δ_{iso} values for $KClO_4$ and $RbClO_4$ which also possess small quadrupole couplings. The lowest chemical shifts are observed for the anhydrous phases, $LiClO_4$, $Mg(ClO_4)_2$, and $Ba(ClO_4)_2$ (i.e., 1029.6 ppm $\leq \delta_{iso} \leq$ 1034.2 ppm), which exhibit the largest quadrupolar couplings of the perchlorates studied. This may indicate that the isotropic chemical shift for the perchlorate anions is more sensitive to distortions of the ClO_4 tetrahedron than effects originating from the cations in the second coordination spheres to the chlorine atom. Finally, it is noted that the quadrupole coupling for $(CH_3)_4NClO_4$ is very similar to the value $C_Q = 0.318$ MHz, reported for trimethylammonium perchlorate at 303 K.[11]

^{37}Cl MAS NMR. To illustrate that the ^{37}Cl isotope is also amenable to solid-state NMR experiments of the central and satellite transitions, Figure 8 shows representative ^{37}Cl MAS NMR spectra of four of the perchlorates, i.e., $LiClO_4$, $Mg(ClO_4)_2 \cdot 6H_2O$, $Ba(ClO_4)_2 \cdot 3H_2O$, and $NaClO_4 \cdot H_2O$. Obviously, these spectra require more scans in order to obtain signal-to-noise ratios similar to those observed in the ^{35}Cl MAS NMR spectra (Figures 2−5) because of the lower natural abundance and lower Larmor frequency for ^{37}Cl compared to ^{35}Cl. The results from the optimized simulations of the experimental spectra in Figure 8 are listed in Table 2, which also includes ^{37}Cl NMR data for $RbClO_4$. Comparison of these data with those obtained for ^{35}Cl (Table 1) reveals that both isotopes give identical isotropic chemical shifts in agreement with earlier reported results for the cubic alkali-metal chlorides from ^{35}Cl/^{37}Cl MAS NMR.[7] Furthermore, within the error limits the quadrupole asymmetry parameters in Table 2 are identical to those determined from ^{35}Cl MAS NMR. The ^{35}Cl C_Q values (Table 1) are on average a factor of 1.26 larger than those for the ^{37}Cl isotope. This factor is in accord with the corresponding ratio of the quadrupole moments for the two isotopes, i.e., $Q(^{35}Cl)/Q(^{37}Cl) = 1.268\,877\,3$.[33]

The centerband observed for the ^{37}Cl central transition of $LiClO_4$ under MAS at 14.1 T (Figure 8a) has a width $W_{MAS}^{^{37}Cl} = 1300$ Hz which is slightly smaller than the width of the corresponding centerband for the ^{35}Cl central transition (1730 Hz), i.e., the ratio of the widths $W_{MAS}^{^{35}Cl}/W_{MAS}^{^{37}Cl} = 1.33$. The width of the centerband under MAS is given by[34]

$$W_{MAS} = \frac{9}{14\nu_L}\left[\frac{C_Q}{2I(2I-1)}\right]^2\left(1+\frac{\eta_Q}{6}\right)^2\left[I(I+1)-\frac{3}{4}\right] \quad (1)$$

where $C_Q = e^2qQ/h$. The theoretically expected increase in second-order quadrupolar broadening for ^{37}Cl, caused by its lower Larmor frequency, is more than compensated for by the smaller quadrupole moment (Q) for ^{37}Cl as compared to the value for ^{35}Cl. From eq 1 we obtain a ratio $W_{MAS}^{^{35}Cl}/W_{MAS}^{^{37}Cl} = 1.34$, i.e., a ratio independent of the magnetic field and in excellent agreement with our experimental observation at 14.1 T. Thus, chlorine quadrupole coupling parameters can in certain

(32) McCullough, J. D. *Acta Crystallogr.* **1964**, *17*, 1067.
(33) Lovas, F. J.; Tiemann, E. *J. Phys. Chem. Ref. Data* **1974**, *3*, 609.
(34) Samoson, A.; Kundla, E.; Lippmaa, E. *J. Magn. Reson.* **1982**, *49*, 350.

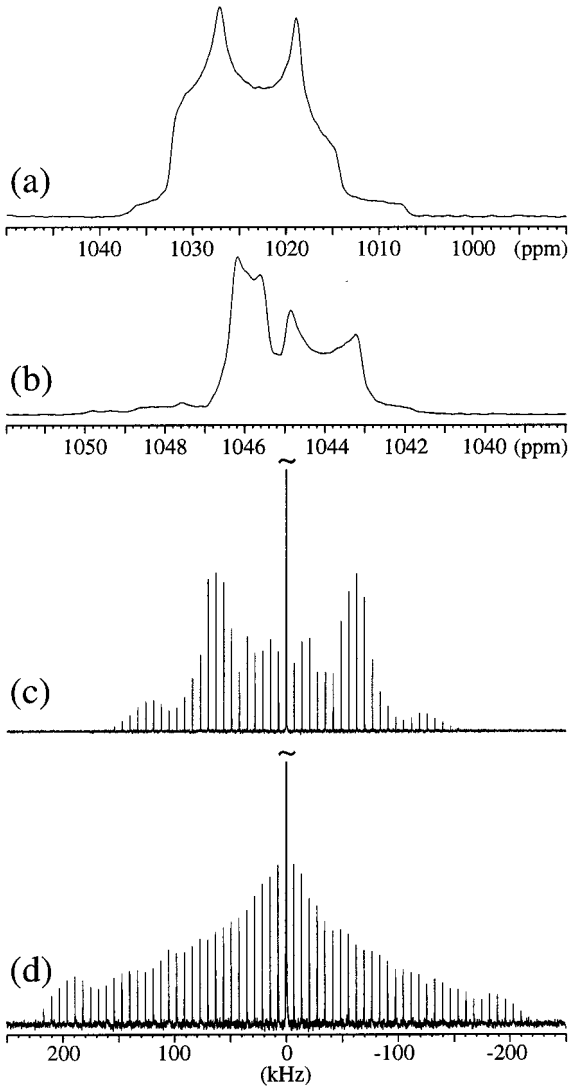

Figure 8. ^{37}Cl MAS NMR spectra of the central transitions for (a) $LiClO_4$ and (b) $Mg(ClO_4)_2 \cdot 6H_2O$ and of the satellite transitions for (c) $Ba(ClO_4)_2 \cdot 3H_2O$ and (d) $NaClO_4 \cdot H_2O$. A spinning speed of $\nu_r = 8.0$ kHz was employed for the spectrum in panel a while the other spectra used $\nu_r = 7.0$ kHz; 16 384 scans were acquired for the spectra in panels a and c while panels b and d employed 11 776 and 15 616 scans, respectively. The central transition in panel c is cut off at $^1/_{10}$ of its total height while it is cut off at $^1/_{18}$ of its height in panel d.

cases be advantageously extracted from ^{37}Cl MAS NMR spectra of the central transition. Such cases include studies of strong quadrupolar interactions, where the highest available spinning speed puts a limit on the observation of an undistorted centerband with no overlap from the first- or higher-order ssbs from the central transition, i.e., $\nu_r > W_{MAS}$. Although the reduced width of the ssb manifolds from the satellite transitions for ^{37}Cl compared to ^{35}Cl favors the observation of the ^{37}Cl isotope, this effect is markedly counteracted by the lower sensitivity (natural abundance, gyromagnetic ratio) for ^{37}Cl and by the increasing baseline distortion as a result of acoustic ringing. Thus, ^{37}Cl MAS NMR of the satellite transitions may primarily serve as an independent test of the validity of C_Q, η_Q, and δ_{iso} parameters obtained from ^{35}Cl MAS NMR.

Conclusions

This work has shown that ^{35}Cl (^{37}Cl) MAS NMR at high magnetic fields represents a valuable tool for characterizing perchlorate anions in inorganic solids. ^{35}Cl quadrupolar couplings (C_Q and η_Q) and isotropic chemical shifts can be determined with high precision from ^{35}Cl MAS NMR spectra of the central or the satellite transitions for inorganic perchlorates. The ^{35}Cl MAS NMR spectra also reveal the number of different perchlorate sites in the asymmetric units while the quadrupole coupling parameters may be related to structural details of the local environments for the perchlorate ions. Since the perchlorates studied are widely used inorganic materials (e.g., in inorganic synthesis and complex chemistry), the ^{35}Cl NMR data determined in this work may serve as useful benchmarks in future ^{35}Cl NMR studies of perchlorates. For selected samples, ^{37}Cl NMR data have also been obtained, giving identical ^{37}Cl and ^{35}Cl isotropic chemical shifts and quadrupole asymmetry parameters and ^{37}Cl quadrupolar coupling constants which are a factor 1.27 smaller than those for the ^{35}Cl isotope. The individual environments for the perchlorate ions are best characterized or distinguished by their ^{35}Cl quadrupole coupling constants since only very small variations in isotropic ^{35}Cl chemical shifts are observed. The ^{35}Cl NMR data for the anhydrous and hydrated perchlorates show that hydration and dehydration processes may be advantageously followed by ^{35}Cl MAS NMR. This may allow for quantitative studies of the hydration kinetics for perchlorate compounds employing variable-temperature ^{35}Cl MAS NMR along with spectral simulations which utilize the ^{35}Cl NMR parameters determined for the pure phases.

Acknowledgment. The use of the facilities at the Instrument Centre for Solid-State NMR Spectroscopy, University of Aarhus, sponsored by the Danish Research Councils (SNF and STVF), Teknologistyrelsen, Carlsbergfondet, and Direktør Ib Henriksens Fond, is acknowledged.

IC9811650